Influence of fiber diameter and surface roughness of electrospun vascular grafts on blood activation

Milleret, Vincent ; Hefti, Thomas ; Hall, Heike ; Vogel, Viola ; Eberli, Daniel

Abstract: Electrospun grafts are widely investigated for vascular graft replacement due to their ease and compatibility with many natural and synthetic polymers. Here, the effect of the processing parameters on the scaffold's architecture and subsequent reactions of partially heparinized blood triggered by contacting these topographies were studied. Degrapol(®) (DP) and poly(lactic-co-glycolic acid (PLGA) electrospun fibrous scaffolds were characterized with regard to fiber diameter, pore area and scaffold roughness. The study showed that electrospinning parameters greatly affect fiber diameter together with pore dimension and overall scaffold roughness. Coagulation cascade activation, early platelet adhesion and activation were analyzed after two hours exposure of blood to the biomaterials. While no differences were found between DP and PLGA with similar topographies, the blood reactions were observed to be dependent on the fiber diameter and scaffold roughness. Scaffolds composed of thin fibers (diameter < 1 m) triggered very low coagulation and almost no platelet adhered. On the other hand, scaffold with bigger fiber diameter (2-3 m) triggered higher thrombin formation and more platelets adhered. The highest platelet adhesion and activations rates as well as coagulation cascade activation were found in blood incubated in contact to the scaffolds produced with the biggest fiber diameter (5 m). These findings might indicate that electrospun grafts with small fiber diameter (<1 m) could perform better with a reduced early thrombogenicity by lower platelets adhesion and lower activation of platelets and coagulation cascade.

DOI: https://doi.org/10.1016/j.actbio.2012.07.032

Influence of fiber diameter and surface roughness of electrospun vascular grafts on blood activation

Vincent Milleret[1]*, Thomas Hefti[1,2,3], Heike Hall[1], Viola Vogel[1] and Daniel Eberli[4]

[1] Cells and Biomaterials, Department of Materials, ETH Zurich, Switzerland;

[2] Thommen Medical AG, Waldenburg, Switzerland

[3] Laboratory for Surface Science and Technology, Department of Materials, ETH Zurich, Zürich, Switzerland

[4] Laboratory for Urologic Tissue Engineering and Stem Cell Therapy, Department of Urology, University Hospital Zurich, Switzerland

* Corresponding author:

Vincent Milleret

ETH Zurich, Department of Materials, HCI E429

Cells and BioMaterials

Wolfgang-Pauli-Strasse 10

CH-8093 Zürich, Switzerland

vincent.milleret@hest.ethz.ch

+41 44 633 69 49 phone

+41 44 632 10 73 fax

Running title: Electrospun vascular graft with decreased blood activation.

Key words: Vascular graft, blood activation, electrospinning, tissue engineering

Figures: 4, Tables: 1

Abstract

Electrospun grafts are widely investigated for vascular graft replacement due to their ease and compatibility with many natural and synthetic polymers. Here, the effect of the processing parameters on the scaffold's architecture and subsequent reactions of partially heparinized blood triggered by contacting these topographies were studied. Degrapol® (DP) and poly(lactic-co-glycolic acid (PLGA) electrospun fibrous scaffolds were characterized with regard to fiber diameter, pore area and scaffold roughness. The study showed that electrospinning parameters greatly affect fiber diameter together with pore dimension and overall scaffold roughness.

Coagulation cascade activation, early platelet adhesion and activation were analyzed after two hours exposure of blood to the biomaterials. While no differences were found between DP and PLGA with similar topographies, the blood reactions were observed to be dependent on the fiber diameter and scaffold roughness. Scaffolds composed of thin fibers (diameter < 1µm) triggered very low coagulation and almost no platelet adhered. On the other hand, scaffold with bigger fiber diameter (2-3 µm) triggered higher thrombin formation and more platelets adhered. The highest platelet adhesion and activations rates as well as coagulation cascade activation were found in blood incubated in contact to the scaffolds produced with the biggest fiber diameter (5µm).

These findings might indicate that electrospun grafts with small fiber diameter (<1µm) could perform better with a reduced early thrombogenicity by lower platelets adhesion and lower activation of platelets and coagulation cascade.

1. Introduction

In Europe, cardiovascular diseases (CVD) are responsible for about 50 % of all mortality causing about 4.3 million deaths per year [1] and in 2008, over 2.6 % of the overall population in Europe was admitted in an hospital for CVD [2]. The restriction of blood flow by arteriosclerosis thus represents a significant medical burden. If detected early, many obstructed blood vessels can be bypassed or replaced by vascular substitutes, including arterial autografts, polytetrafluoroethylene (ePTFE) and polyester grafts [3].

Autografts were observed to be the most successful choice for the repair of smaller diameter vascular grafts with primary patency rates of 73 % compared to 47 % for ePTFE and 54 % for polyester grafts [4]. The main limitation of autologous grafts is their availability and donor site morbidity [3]. Therefore, tissue engineered vascular grafts (TEVG) using autologous cells are promising alternatives. While large diameter TEVG grafts regenerated successfully in humans with a five-years patency of about 90 % [5], small diameter vascular grafts (diameter < 5 mm) are still a challenge [6]. Among the main reasons for graft failure of small diameter grafts (anastomotic intimal hyperplasia, aneurysm formation, infection, and progression of atherosclerotic disease), acute thrombogenicity of the graft is one of the most important [7-9].

Reduction of thrombogenicity is crucial for improving the graft success rate, and several strategies have been developed with partial success. The most studied graft surface modifications consist in the addition of anti-thrombotic factors, coating with cell-adhesion ligands to promote endothelialization or seeding with endothelial cells. Nevertheless, addition of soluble anti-thrombotic factors has a time limited activity, which eventually stops when the whole drug supply is used up. Coating with cell

adhesive ligands and seeding with endothelial cells both aim at a better endothelialization, which provides excellent anti-thrombogenic properties [10]. However, coating with cell adhesion ligands remains unspecific to endothelial cells and also supports platelets and smooth muscle cells adhesion, leading to clotting and subsequent pseudointimal thickening [3]. Also, *in vitro* endothelialization cannot guaranty full coverage of the graft and cells are lost during transplantation, therefore complete endothelialization *in vivo* is not instantaneous and takes at least 10 days [11], thus acute thrombogenicity cannot be fully prevented by this strategy.

Electrospinning has been widely used as a processing method for the design of vascular grafts [12, 13] with performances equal or superior to current standard, ePTFE [14]. This technique is quite popular as it allows easy production of fibrous tubular scaffolds with controllable composition, architecture, fiber diameter and mechanical properties [12, 15, 16]. Scaffold properties tremendously affect the reaction of contacting cells and tissues; for instance, scaffold porosity affects the cell infiltration *in vitro* [15, 16] and tissue integration *in vivo* [17] and fiber orientation can affect cell alignment [18]. Regarding vascular grafts, a number of studies showed that endothelialization on scaffolds with nano-fibers would be improved compared to micro-fiber scaffolds [12, 19].

Although early thrombosis has been recognized as a major cause of graft occlusion, no study has investigated the influence of electrospun graft topography on acute thrombogenicity. In the presented study, two polymers – DegraPol® (DP), which has been shown to meet essential requirements for vascular grafts such as good biocompatibility [20], mechanical properties [16] and hemocompatibility [21], as well as FDA-approved poly(lactic-co-glycolic acid) (PLGA), which has been widely exploited

for many biomedical applications [22-25], were processed into scaffolds with defined fiber diameters. We subsequently evaluated the effects of fiber diameters and of resulting surface topography of the electrospun scaffolds on the early coagulation, platelet adhesion and activation. The blood coagulation cascade can be activated by a specific stimulus such as injury or exposure to a thrombogenic surface. A key enzyme required for the activation of the cascade is thrombin triggering the polymerization of fibrinogen into fibrin fibrils [26, 27]. Thrombin-antithrombin (TAT) complexes have been used as a surrogate marker for thrombin generation [28] and were used in this study as a marker for coagulation cascade activation. The aim of this contribution is to understand the effect of the scaffolds architecture on the blood reaction in order to be able to design a scaffold with minimal acute thrombogenicity.

2. Materials and methods

2.1 Polymers

The polyester-urethane (trade name DegraPol® (Mw = 70 kDa)) was produced according to the procedure described by [29, 30]. The poly(lactic acid-*co*-glycolic acid) (Resomer®, PLGA, Type RG 85:15, Mw = 280 KDa) was obtained from Boehringer Ingelheim, Germany. Chloroform (stabilized with ethanol) was obtained from Emanuele Centonze SA, Switzerland and Hexa-fluoro Propanol (HFP) was purchased by Sigma.

2.2 Scaffold production by electrospinning and solvent casting

Fibrous scaffolds were produced with an electrospinning setup, assembled in-house and which consisted of a syringe pump (Racel Scientific Instruments Inc., USA), a spinning head consisting of a central stainless steel tube, a hollow cylindrical rotating aluminum mandrel for fiber collection (length: 100 mm, diameter: 80 mm, wall thickness: 5 mm) and a DC high voltage supply (Glassman High Voltage Inc., USA).

Homogeneous DegraPol solutions were prepared by letting the desired amount of polymer dissolve in a HFP-chloroform mixture (wt % 25 : 75) at room temperature (RT) overnight, while PLGA solutions were dissolved in chloroform only. The homogeneous solutions were loaded into a 2 mL syringe (B. Braun Melsungen AG, Germany) and pumped into the spinning heads. Electrospinning parameters, such as the polymer concentration, the distance between the spinning head and the collecting mandrel (referred to as working distance), the flow rate and the applied voltage between the spinning head and the collector, were set for producing electrospun scaffolds with three different desired diameter, called ES1, ES2 and ES3 and summarized in Table 1.

Uniform smooth polymeric films were used as plain controls to the porous electrospun fibrous scaffolds. For production of polymeric films used as controls, a wt 30 % DegraPol solution and a wt 10 % PLGA solution (in chloroform) were prepared. The solutions were then cast using a stencil with a 500 µm gap on a polytetrafluoroethylene-coated plate. The films were left under a fume hood until complete evaporation of the solvent. The so-produced casted scaffolds are referred as CS throughout the manuscript.
Out of the polymeric scaffolds, disks of 20 mm diameter were punched out and used for blood incubation experiments.

2.3 Scaffold characterization

Fiber diameters were measured as described [18] using SEM micrographs: first a diagonal line was drawn from bottom left to top right of the image and the fiber diameter was measured, perpendicular to the fiber length, at the points where the line crossed the fiber using ImageJ (http://rsbweb.nih.gov/ij/) after calibration with the scale bar of the microscope image. The diameters of the fibers were averaged over all the images of a sample (50 fiber diameters measured per sample). Pore area was determined as described [12] using SEM micrographs and manually approximating the surface pores (50 pores measured per sample).
Surface roughness was measured by means of stereo-SEM, where a surface is imaged twice with conventional SEM, eucentricly tilted (i.e. in the focus plane) by 10° [31]. From these two images of the same region of interest 3D information of the surface topography was calculated by means of automatic image correlation with specialized software (MeX, Alicona, Graz, Austria)[32]. Resulting height profiles were evaluated using the window-roughness method, where values above a certain cut-off wavelength λ_c

are identified as waviness and are not included in the surface roughness calculation [33]. Here, cut-off wavelength was set at λ_c = 200 µm and surface roughness was expressed as R_a, describing the arithmetic average of the absolute values in z-direction.

Water contact angle was measured using the Ramé-Hart model 100 (Ramé Hart Inc, Moutain lakes, NJ, USA) at room temperature. Water drops of 5 µL were used for water contact angle measurements in air.

2.4 Partially heparinized whole human blood

Human whole blood from healthy volunteers not taking medication was purchased from the local blood bank (Zentrale Blutbank, University Hospital Zürich) and was heparinized directly upon withdrawal by using 5 mL vacutainer tubes (BD Vacutainer™ No Additive (Z) Plus Tubes) modified with 15 IU sodium heparin (Carl Roth, Karlsruhe, Germany, Eur. Ph., 120 IU/mg) resulting in a final concentration of 3 IU heparin/mL blood (as proposed in [31]). All blood samples used for the experiments were freshly withdrawn, transported and stored at room temperature and were used within 2 hours.

2.5 Slide chamber, blood incubation and preparation of samples

Polymeric scaffolds were incubated with partially heparinized whole human blood within a rotating slide chamber similar to one described earlier [34]. In brief polymeric scaffolds were assembled on both sides of a Teflon ring of 12 mm inner diameter and 10 mm height and clamped between two stainless steel plates creating a circular chamber with a final volume of 1.1 mL. The closed chambers were filled with blood through a syringe

port and incubated for 10 minutes or 2 hours under rotation at 6.6 rpm in an incubator (B6030, Heraeus, Hanau, Germany) at 37 °C.

2.6 Enzyme linked immunoassays (ELISA) for the detection of Thrombin-antithrombin (TAT)

For analysis of TAT before and after incubation the blood was collected and EDTA was added to a final concentration of 5 mM. Subsequently the blood was centrifuged for 10 minutes at 2'000 g at room temperature and the supernatants were stored at -20 °C until further analysis.

Concentrations of TAT complexes were determined using commercially available ELISA kits (AssayMax Human Thrombin-antithrombin (TAT) Complexes). The assay was carried out according to the manufacturer's instructions and with reagents provided by the manufacturers. Blood incubated with sand blasted titanium (as described by [35]) disks were used as positive control. The experiments were performed at least 4 times in duplicates.

2.7 Scanning electron microscopy (SEM)

Scaffolds were analyzed by SEM before and after 10 min and 2 h of incubation in heparinized (3 IU/mL) whole human blood at 37 °C. Briefly, following blood incubation, samples were carefully rinsed 3 times in PBS (Sigma) and fixed in 3 % glutaraldehyde in PBS for 30 minutes, followed by 2 % osmiumtetroxid in PBS for 20 minutes, both at RT. Samples were subsequently dehydrated in a graded series of ethanol (from 30 % to 96 %). Out of absolute ethanol the samples were dried over the critical point of CO_2 (Tk =

31.8 °C, Pk = 73.8 bar) using a critical-point dryer (CPD 030 Critical Point Dryer, Bal-Tec AG, Balzers, Liechtenstein). The samples were sputter-coated with 7 nm platinum and the images were recorded with a Zeiss SUPRA 50 VP at 10 kV using secondary electron signals.

Stereo-SEM analysis was performed on all samples, the same ROI being imaged twice with the stage eucentricly tilted by 10° between the two images. From these pairs of images, 3D data were calculated by means of specialized software (MeX from Alicona, Graz Austria).

2.8 Confocal laser scanning microscopy (CLSM)

For confocal laser-scanning microscopy of deposited blood components, blood-exposed scaffolds with different topographies were carefully rinsed 3 times in PBS and subsequently fixed for 20 minutes in an aqueous solution of 4 % (w/v) PFA, 65 mM PIPES, 25 mM HEPES, 10 mM EGTA and 3 mM $MgCl_2$ and subsequently incubated for 10 minutes in PBS containing 0.1 % Triton X 100 (500 µL per well) for cell permeabilization. On all samples, cell nuclei were stained with 1:2000 Hoechst 33342 (Molecular Probes) in PBS containing 1 % (w/w) of BSA (Bovine Serum Albumin, SAFC, USA) for 10 minutes at RT. Staining of the actin cytoskeleton was achieved by incubating the samples in a solution of Alexa Fluor® 488-phalloidin (1:200, Molecular Probes) in 1 % (w/w) of BSA in PBS for 2 hours at RT.

P-Selectin was carried out by incubating the samples in solutions of purified anti-human CD62P – P-Selectin (Biolegend, No 304902) using 1:50 dilutions for 2 hours followed by incubation in a solution of anti-mouse Alexa 633 (1:200, Molecular Probes) for 1 hour at

RT. Samples were washed 3 times with PBS after incubation with antibody solutions. All antibodies were diluted in 1 % (w/w) BSA in PBS. Samples were mounted on glass coverslips (24 x 50 mm, Carl Roth, Karlsruhe, Germany) using Mowiol 4-88 mounting media (Calbiochem, Damstadt, Germany), left overnight and analyzed by laser scanning confocal microscopy (SP5, Leica Microsystems, Germany). Fluorescence was analyzed using the following wavelengths: Hoechst 33342 (ex = 350 nm and em= 440 nm), Alexa-488 (ex = 495 nm and em = 519 nm) and Alexa-633 (ex = 632 nm and em = 647 nm).

2.9 Statistical analysis

All mean values were compared by two-way ANOVA analysis using Matlab 7.9 (the MathWorks Inc, USA). Statistical significance was accepted for $p < 0.05$ after comparing the mean values by Bonferroni *post hoc* test and was designated by an asterisk. Trendlines and fitting in Figure 1j and 2k were also calculated with Matlab. Throughout the manuscript the data is presented as a mean ± standard deviations.

3. Results

3.1 Morphology, roughness and wettability of the DegraPol scaffolds

Scaffolds with 3 defined fiber diameter and surface architecture were produced by electrospinning and referred as ES1, ES2 and ES3. Figure 1 represents SEM micrographs showing the morphology of the DegraPol (Figure 1 a-d) and PLGA (Figure 1 e-h) surfaces. The fiber diameters of the different scaffolds are shown in Figure 1 i. In brief, on the solvent cast films (Figure 1 a and e) no fiber diameter was measured, ES1 scaffolds had an average diameter below one micrometer (0.93 ± 0.33 µm for DP and 0.63 ± 0.09 µm for PLGA, Figure 1 b and f respectively), while ES2 scaffolds were comprised between 2 and 3 µm (2.67 ± 0.63 µm for DP and 2.06 ± 0.31 µm for PLGA, Figure 1 c and g respectively). Lastly, ES3 scaffolds for DP were composed of fibers with a mean diameter of 6.52 ± 1.53 µm, while PLGA showed a mean diameter of ES3 5.02 ± 0.75 µm (Figure 1 d and h respectively). No significant difference was found between DP and PLGA (for CS, ES1, ES2 and ES3), while the different classes of scaffold were significantly different from each other (see Figure 1 i). Areas of the surface pores were calculated and reported in Figure 1 j. Casted scaffolds (CS) not having fibers, no pore was determined for these scaffolds, pores on fibrous scaffolds increased with the diameter, for both DegraPol scaffolds (for which ES1, ES2 and ES3 had mean pore areas of 43 ± 29 μm^2, 368 ± 208 μm^2 and 1623 ± 858 μm^2, respectively) as for PLGA scaffolds (for which the pore areas increased from 33.9 ± 20 μm^2 for ES1, to 226 ± 147 μm^2 for ES2 and finally 988 ± 779μm^2 for ES3). Nevertheless, no differences in pore area were found between DP and PLGA scaffolds for similar fiber diameters (Figure 1 j). In

addition, the pore area of the scaffolds, seem to vary in a quadratic way compared to the fiber diameter, as the R^2 value with a quadratic trend line fit was 0.993 (Figure 1 k).

Roughness of the scaffolds was assessed by analysis of stereo-SEM pairs (Figure 2 a-h), the surface roughness R_a of the scaffolds was found to increase with the diameter of the constituting fibers. Solvent casted scaffolds were found to be the smoothest with a roughness of 0.36 ± 0.01 µm for DP and 0.42 ± 0.05 µm for PLGA, followed by ES1 scaffolds, 1.46 ± 0.08 µm for DP and 1.50 ± 0.07 for PLGA, ES2 scaffolds, 3.90 ± 0.27 µm for DP and 3.94 ± 0.08 for PLGA, and finally ES3 scaffolds had the highest R_a values (6.26 ± 0.69 µm for DP and 5.00 ± 0.21 for PLGA). Scaffold roughness was found to be dependent on processing conditions, but independent of the polymer used (Figure 2 i). Fitting the roughness-diameter curve for both PLGA and DP, R^2 value with a linear trendline fit was 0.902 (Figure 2 j).

Water contact angle of all polymeric scaffolds were measured (Table 2). While no significant difference was found between PLGA and DP, processing parameters affect the scaffold wettability. The CS were found to be much less hydrophobic than the other scaffolds (73.1 ± 2.6 ° and 76.6 ± 13.1 ° for DP ad PLGA respectively). The scaffolds with the smallest fibers were found to be a little bit more hydrophobic (128.6 ± 4.2 ° for DP and 122.8 ± 3.5 ° for PLGA) than ES2 and ES3 (all comprised between 116.3 ± 5.3 and 118.7 ± 1.9 °).

3.2 Blood activation by the different polymeric scaffolds

To analyze the differences between the adhesion and activation of platelets depending on the surface characteristics, namely fiber diameter and pore size, the different scaffolds, after incubation in blood, were characterized by confocal laser-scanning microscopy after

staining with specific antibodies, while the blood was tested for TAT levels as indicators of coagulation cascade activation, after 2 hrs of incubation with whole blood.

Platelet adhesion and activation in the blood clots were analyzed by (immuno-)stainings of a platelet surface marker CD62p, the actin cytoskeleton and cell nuclei on the polymeric surfaces. The total quantity of cells was determined by nuclear staining while the antibody against CD62p was used to stain persistently activated platelets. Figure 4 A-H show projections of z-stacks obtained by confocal laser-scanning microscopy images of blood clots formed on polymer cast- and electrospun scaffolds.

The surface coverage by activated CD62p-positive platelets as well as the ratio of activated versus nonactivated platelets is indeed greatly affected by the topography of the scaffold (Figure 4 i and j). Independent of the polymer used, the overall coverage by platelets was increased on electrospun scaffolds with increasing fiber diameter. For DP (Figure 4 i), total coverage was increasing from ES1 – 4.5 ± 2.5 %, to ES2 – 19.7 ± 12.6 %, until maximal values for ES 3 of 45.8 ± 13.0 %. In a similar manner, ES1, ES2 and ES 3 PLGA scaffolds were covered at 4.2 ± 0.7 %, 15.8 ± 2.5 % and 36.0 ± 7.0 % respectively (Figure 4 i). No difference between DP and PLGA electrospun scaffolds were found. The solvent cast scaffolds were found to be comparable to ES1 for DP and PLGA scaffolds.

For platelet activation, no difference could be found comparing DP to PLGA scaffolds (Figure 4 j). For both polymers, the activation remained lower for CS, ES1 and ES2 (respectively 1.2 ± 0.9 %, 1.0 ± 0.8 % and 1.6 ± 1.9 % for DP and 0.5 ± 0.2 %, 1.0 ± 0.2 % and 1.2 ± 0.6 % for PLGA); while it was significantly increased in ES3 (13.4 ± 5.3 % for DP and 14.8 ± 3.5 % for PLGA).

Thrombin-antithrombin complexes indicate an activated coagulation cascade and are correlated to the extent of blood activation. TAT levels in blood were not different if exposed to PLGA or DegraPol (Figure 4). Concerning the effect of surface topography, the protein levels in blood incubated with the two smoothest surfaces (CS and ES1) were not increased compared to before activation (14.1 ± 2.9 ng/mL). Rougher surfaces triggered an increase in TAT complexes; for ES2 surfaces values increased significantly to 24.4 ± 9.8 ng/mL for DegraPol scaffolds and 24.9 for PLGA ones. Even higher values were measured for the roughest surfaces of ES3 (57.1 ± 19.8 ng/mL for DP and 36.0 ± 10.4 ng/mL for PLGA).

4. Discussion

Designing blood contacting medical devices in general, and vascular grafts in particular, has to consider how to up- or down-regulate blood-material reactions to prevent adverse reactions or failure. In case of small diameter TEVG by electrospinning, early thrombus formation often causes graft failure. Studies have aimed at improving the thrombogenicity of TEVG by changing the surface properties [36, 37], adding antithrombotic drugs [36, 38], or growing an endothelium on the graft prior to implantation [39, 40]. Although electrospun vascular scaffolds with fiber diameters varying from couple of hundreds of nm [12] up to 6 µm [41], *in vitro* and from about 500 nm [42] to over 3 µm [43] *in vivo* were used in recent publications, the effect of fiber diameter and their topography on thrombogenicity was never addressed. For this purpose, electrospun scaffolds of DegraPol and PLGA were produced and characterized with various defined fiber diameters. It is known and here confirmed that fiber diameter dictates other surface properties, as the pore size [12, 44] and the surface roughness [45] increase with increasing constituting fiber diameter.

While assessing the thrombogenicity of the defined scaffold varying in chemistry and topography, our major finding is that the blood reaction, namely platelet adhesion and activation, is far more affected by the scaffold morphology than by differences in the polymers chemistries used (Figure 3 and 4).

For similar scaffold morphologies (i.e. constituting fiber diameter) DegraPol and PLGA performed in a similar way. DegraPol and PLGA flat surfaces were already shown to

trigger comparable changes in protein levels in blood [21]. More in details, when analyzing the protein levels in blood after 2 hours exposure to flat surfaces of PLGA and DegraPol, no differences were found in blood activation in terms of coagulation cascade activation (evaluating TAT levels), complement system activation (C5a levels) and, more interestingly, platelet activation (PF4 levels) [21]. Similar activation on DP and PLGA surfaces, could be explained by their comparable hydrophilicity (as already reported in the literature for DP films: 65 - 79° (Henry et al., 2006) and PLGA films contact angle: 72 ± 3° [46]), which influences thrombogenicity [47]. This emphasizes furthermore the importance of the scaffold topography in thrombogenicity of the construct.

Interestingly and to our knowledge never described before, coagulation cascade, platelet adhesion and activation were observed to depend on the average fiber diameter of the scaffold. Scaffolds with fibers smaller than 1µm induced a lower coagulation cascade activation and platelet adhesion when compared to scaffolds composed of bigger fibers. Our findings with electrospun fibers thus agree with conclusion derived from utilizing other types of surface topographies: it has been widely observed that platelet adhesion and blood reaction both depend on surface roughness [48-52], and that platelet adhesion and blood activation are also affected by other defined surface topographies, i.e. pillars [53], lenses [54] and struts [55]. All the data taken together suggests that reducing the size of surface features (pillars, lenses, struts, or here fibers) might lead to a reduction of the contacting blood activation. Still, not only the size of the surface features matters, but also their aspect ratio, distribution and packing density [53]. Concerning electrospun fibers, aspect ratio doesn't vary with fiber diameter, but to some extent, it is possible to adjust the fiber distribution and density [56]. This could be an additional way of tuning

the thrombogenicity of electrospun fibers. Other properties of the scaffold might play a role in differential blood activation with changing fiber diameter. Indeed, scaffold wettability is also affected by fiber diameter and roughness in general. In accordance, with Cui et al, scaffolds with smaller fibers were found to be a little bit more hydrophobic than scaffolds with bigger fibers [57]. Nevertheless, CS and ES1 (which have equivalent roughness) are respectively the most hydrophilic and most hydrophobic scaffolds tested in the present study and are still performing similarly in terms of thrombogenicity. This emphesizes that wettability alone cannot explain the presented results, and that roughness changes very likely are responsible for differential blood activation.

Exploiting electrospinning to alter surface topographies has the advantage that it is relatively easy to control the processing parameters to tune fiber diameters, and is far cheaper than producing micro- or nanofabricated materials. Straightforward and cheap to produce, solvent casted films were used as controls due to their low roughness and good reproducibility. Throughout the experiments, they showed very good performance in terms of blood activation, which could imply that solvent casted films could also be good candidates to reduce thombogenicity. However, their major disadvantage remains the lack of porosity, crucial for exchanges between the different layers, nutrient supply or chemical signaling from endothelial cells that guide organization of the growth and development of connective tissue cells that form the surrounding layers [58]. While reducing thrombogenicity, electrospun scaffolds with submicrometer-fibers have a limited cell infiltration [12, 59], which is a requirement for functional vascular substitute with a good tissue integration and healthy smooth muscle cell layer. Therefore, sub-

micrometer fibers are not suited for muscle layer development, and several strategies were developed for increasing the pore size of electrospun scaffolds, including salt leaching, use of sacrificial fibers, ice crystals as void templates, or gas foaming (reviewed in [60]). Scaffolds with greater pore sizes were observed to support enhanced smooth muscle cell infiltration compared to denser scaffold and are therefore better suited for supporting the muscle layer formation [12]. In addition, mechanical properties of scaffold with thinner diameter have reduced mechanical properties, possibly affecting the graft stability [15]. An optimize graft should contain at least another layer promoting muscle layer formation and graft stability.

5. Conclusion

Vascular grafts should display two main features: acute thrombogenicity should not only be avoided, but it should also promote a good tissue regeneration for full function recovery. Two parts of the vessel are key for its functionality: the endothelium that actively interacts with blood and the smooth muscle layer providing contractility to the organ. Our finding that electrospun scaffold fibers with increasing diameter showed an increase in platelet adhesion and activation, and coagulation cascade activation *in vitro* now suggests a new avenue how to improve upon electrospun scaffold designs. Although *in vivo* experiments should be carried out to confirm the results of our *in vitro* model, electrospun vascular graft should probably be composed from multiple layers: an inner layer being less thrombogenic and supporting a more rapid endothelialization, and an outer layer promoting an improved surrounding tissue integration and providing mechanical stability to the graft. Indeed, the endothelial cell function, spreading and

proliferation were observed to be enhanced on sub-micrometer fibers [12, 19, 45, 61, 62]. At least for endothelial cells, it was reported that they adhered and proliferated better on thinner fibers compared to microfibers, and that cells on sub-micrometer, to 1.2 µm fibers spread while they remained round-shaped and non-proliferating on 7 µm diameter fibers [19]. Those results suggest that scaffolds with sub-micrometer fibers might support a faster endothelialization.

6. Acknowledgment

The authors would like to thank the ETH Zurich for funding, and ab medica spa for kindly providing DegraPol® and a research fellowship to V. M.

7. References

[1] Stehouwer CD, Clement D, Davidson C, Diehm C, Elte JW, Lambert M, et al. Peripheral arterial disease: a growing problem for the internist. Eur J Intern Med. 2009;20:132-8.
[2] Allender S, Scarborough P, Peto V, Rayner M, Leal J, Luengo-Ferandez R, et al. European cardiovascular disease statistics. European Heart Network; 2008.
[3] Teebken OE, Wilhelmi M, Haverich A. [Tissue engineering for heart valves and vascular grafts]. Chirurg. 2005;76:453-66.
[4] Mamode N, Scott RN. Graft type for femoro-popliteal bypass surgery. Cochrane Database Syst Rev. 2000:CD001487.
[5] Brewster DC. Current controversies in the management of aortoiliac occlusive disease. J Vasc Surg. 1997;25:365-79.
[6] Klinkert P, Post PN, Breslau PJ, van Bockel JH. Saphenous vein versus PTFE for above-knee femoropopliteal bypass. A review of the literature. Eur J Vasc Endovasc Surg. 2004;27:357-62.
[7] Cho SW, Lim JE, Chu HS, Hyun HJ, Choi CY, Hwang KC, et al. Enhancement of in vivo endothelialization of tissue-engineered vascular grafts by granulocyte colony-stimulating factor. J Biomed Mater Res A. 2006;76:252-63.
[8] Isenberg BC, Williams C, Tranquillo RT. Small-diameter artificial arteries engineered in vitro. Circ Res. 2006;98:25-35.
[9] McClure MJ, Sell SA, Simpson DG, Walpoth BH, Bowlin GL. A three-layered electrospun matrix to mimic native arterial architecture using polycaprolactone, elastin, and collagen: a preliminary study. Acta Biomater. 2010;6:2422-33.
[10] Bunting S, Moncada S, Vane JR. Antithrombotic properties of vascular endothelium. Lancet. 1977;2:1075-6.
[11] Dilley RJ, McGeachie JK, Prendergast FJ. Experimental vein grafts in the rat: re-endothelialization and permeability to albumin. Br J Surg. 1983;70:7-12.
[12] Ju YM, Choi JS, Atala A, Yoo JJ, Lee SJ. Bilayered scaffold for engineering cellularized blood vessels. Biomaterials. 2010;31:4313-21.
[13] Lee SJ, Yoo JJ, Lim GJ, Atala A, Stitzel J. In vitro evaluation of electrospun nanofiber scaffolds for vascular graft application. J Biomed Mater Res A. 2007;83:999-1008.
[14] Pektok E, Nottelet B, Tille JC, Gurny R, Kalangos A, Moeller M, et al. Degradation and healing characteristics of small-diameter poly(epsilon-caprolactone) vascular grafts in the rat systemic arterial circulation. Circulation. 2008;118:2563-70.
[15] Baker BM, Gee AO, Metter RB, Nathan AS, Marklein RA, Burdick JA, et al. The potential to improve cell infiltration in composite fiber-aligned electrospun scaffolds by the selective removal of sacrificial fibers. Biomaterials. 2008:29: 2348-58.
[16] Milleret V, Simona B, Neuenschwander P, Hall H. Tuning electrospinning parameters for production of 3D-fiber-fleeces with increased porosity for soft tissue engineering applications. Eur Cell Mater. 2011;21:286-303.
[17] Leong MF, Rasheed MZ, Lim TC, Chian KS. In vitro cell infiltration and in vivo cell infiltration and vascularization in a fibrous, highly porous poly(D,L-lactide) scaffold

fabricated by cryogenic electrospinning technique. J Biomed Mater Res A. 2009;91:231-40.
[18] Baker SC, Atkin N, Gunning PA, Granville N, Wilson K, Wilson D, et al. Characterization of polystyrene scaffolds for three-dimensional in vitro biological studies. Biomaterials. 2006:27: 3136-46.
[19] Kwon IK, Kidoaki S, Matsuda T. Electrospun nano- to microfiber fabrics made of biodegradable copolyesters: structural characteristics, mechanical properties and cell adhesion potential. Biomaterials. 2005;26:3929-39.
[20] Danielsson C, Ruault S, Simonet M, Neuenschwander P, Frey P. Polyesterurethane foam scaffold for smooth muscle cell tissue engineering. Biomaterials. 2006;8:1410-5.
[21] Milleret V, Simonet M, Bittermann AG, Neuenschwander P, Hall H. Cyto- and hemocompatibility of a biodegradable 3D-scaffold material designed for medical applications. J Biomed Mater Res B Appl Biomater. 2009:91:109-21.
[22] Kim K, Yu M, Zong X, Chiu J, Fang D, Seo YS, et al. Control of degradation rate and hydrophilicity in electrospun non-woven poly(D,L-lactide) nanofiber scaffolds for biomedical applications. Biomaterials. 2003;24:4977-85.
[23] Katti DS, Robinson KW, Ko FK, Laurencin CT. Bioresorbable nanofiber-based systems for wound healing and drug delivery: optimization of fabrication parameters. J Biomed Mater Res B Appl Biomater. 2004;70:286-96.
[24] Bashur CA, Dahlgren LA, Goldstein AS. Effect of fiber diameter and orientation on fibroblast morphology and proliferation on electrospun poly(D,L-lactic-co-glycolic acid) meshes. Biomaterials. 2006;27:5681-8.
[25] Xin X, Hussain M, Mao JJ. Continuing differentiation of human mesenchymal stem cells and induced chondrogenic and osteogenic lineages in electrospun PLGA nanofiber scaffold. Biomaterials. 2007;28:316-25.
[26] Kita R, A. Ti, Kaibara M, Kubota K. Formation of fibrin gel in fibrinogen-thrombin system: static and dynamic light scattering study. Biomacromolecules. 2002;3(5):1013-20.
[27] Kubota K, Kogure H, Masuda Y, Toyama Y, Kita R, Takahashi A, et al. Gelation dynamics and gel structure of fibrinogen. Colloids Surf B Biointerfaces. 2004;38(3-4):103-9.
[28] Diquélou A, Lemozy S, Dupouy D, Boneu B, Sakariassen K, Cadroy Y. Effect of blood flow on thrombin generation is dependent on the nature of the thrombogenic surface. Blood. 1994;84(7):2206-13.
[29] Lendlein A, Colussi M, Neuenschwander P, Suter UW. Hydrolytic degradation of Phase-segregated multiblock copoly(ester-urethane)s containing weak links. Macromol Chem Phys. 2001:202: 2702-11.
[30] Lendlein A, Neuenschwander P, Suter UW. Tissue-compatible multiblock copolymers for medical applications, controllable in degradation rate and mechanical properties. Macromol Chem Phys. 1998:199: 2785–96.
[31] Richards RG, Wieland M, Textor M. Advantages of stereo imaging of metallic surfaces with low voltage backscattered electrons in a field emission scanning electron microscope. J Microsc. 2000;199 (Pt 2):115-23.
[32] Hefti T, Frischherz M, Spencer ND, Hall H, Schlottig F. A comparison of osteoclast resorption pits on bone with titanium and zirconia surfaces. Biomaterials. 2010;31:7321-31.

[33] Wieland M, Hanggi P, Hotz W, Textor M, Keller BA, Spencer ND. Wavelength-dependent measurement and evaluation of surface topographies: application of a new concept of window roughness and surface transfer function. Wear. 2000;237:231-52.
[34] Hong J, Ekdahl KN, Reynolds H, Larsson R, Nilsson B. A new in vitro model study interaction between whole blood and biomaterial. Studies of platelet and coagulation activation and effect of the aspirin. Biiomaterials. 1998:20: 603-11.
[35] Milleret V, Tugulu S, Schlottig F, Hall H. Alkali treatment of microrough titanium surfaces affects macrophage/monocyte adhesion, platelet activation and architecture of blood clot formation. Eur Cell Mater. 2011;21:430-44; discussion 44.
[36] Tepe G, Schmehl J, Wendel HP, Schaffner S, Heller S, Gianotti M, et al. Reduced thrombogenicity of nitinol stents--in vitro evaluation of different surface modifications and coatings. Biomaterials. 2006;27:643-50.
[37] De Scheerder I, Verbeken E, Van Humbeeck J. Metallic surface modification. Semin Interv Cardiol. 1998;3:139-44.
[38] Stahli BE, Camici GG, Tanner FC. Drug-eluting stent thrombosis. Ther Adv Cardiovasc Dis. 2009;3:45-52.
[39] Sarkar S, Sales KM, Hamilton G, Seifalian AM. Addressing thrombogenicity in vascular graft construction. J Biomed Mater Res B Appl Biomater. 2007;82:100-8.
[40] Bordenave L, Remy-Zolghadri M, Fernandez P, Bareille R, Midy D. Clinical performance of vascular grafts lined with endothelial cells. Endothelium. 1999;6:267-75.
[41] Xu F, Cui FZ, Jiao YP, Meng QY, Wang XP, Cui XY. Improvement of cytocompatibility of electrospinning PLLA microfibers by blending PVP. J Mater Sci Mater Med. 2009;20:1331-8.
[42] Innocente F, Mandracchia D, Pektok E, Nottelet B, Tille JC, de Valence S, et al. Paclitaxel-eluting biodegradable synthetic vascular prostheses: a step towards reduction of neointima formation? Circulation. 2009;120:S37-45.
[43] Nottelet B, Pektok E, Mandracchia D, Tille JC, Walpoth B, Gurny R, et al. Factorial design optimization and in vivo feasibility of poly(epsilon-caprolactone)-micro- and nanofiber-based small diameter vascular grafts. J Biomed Mater Res A. 2009;89:865-75.
[44] Telemeco TA, Ayres C, Bowlin GL, Wnek GE, Boland ED, Cohen N, et al. Regulation of cellular infiltration into tissue engineering scaffolds composed of submicron diameter fibrils produced by electrospinning. Acta Biomaterialia. 2005;1:377-85.
[45] Xu C, Yang F, Wang S, Ramakrishna S. In vitro study of human vascular endothelial cell function on materials with various surface roughness. J Biomed Mater Res A. 2004;71:154-61.
[46] Kumbar SG, Nukavarapu SP, James R, Nair LS, Laurencin CT. Electrospun poly(lactic acid-co-glycolic acid) scaffolds for skin tissue engineering. Biomaterials. 2008;29:4100-7.
[47] Hong J, Kurt S, Thor A. A Hydrophilic Dental Implant Surface Exhibit Thrombogenic Properties In Vitro. Clin Implant Dent Relat Res. 2011.
[48] Hecker JF, Scandrett LA. Roughness and thrombogenicity of the outer surfaces of intravascular catheters. J Biomed Mater Res. 1985;19:381-95.
[49] Hecker JF, Edwards RO. Effects of roughness on the thrombogenicity of a plastic. J Biomed Mater Res. 1981;15:1-7.

[50] Park JY, Gemmell CH, Davies JE. Platelet interactions with titanium: modulation of platelet activity by surface topography. Biomaterials. 2001;22:2671-82.
[51] Minelli C, Kikuta A, Tsud N, Ball MD, Yamamoto A. A micro-fluidic study of whole blood behaviour on PMMA topographical nanostructures. J Nanobiotechnology. 2008;6:3.
[52] Kammerer PW, Gabriel M, Al-Nawas B, Scholz T, Kirchmaier CM, Klein MO. Early implant healing: promotion of platelet activation and cytokine release by topographical, chemical and biomimetical titanium surface modifications in vitro. Clin Oral Implants Res. 2010.
[53] Koh LB, Rodriguez I, Venkatraman SS. The effect of topography of polymer surfaces on platelet adhesion. Biomaterials. 2010;31:1533-45.
[54] Chen H, Song W, Zhou F, Wu Z, Huang H, Zhang J, et al. The effect of surface microtopography of poly(dimethylsiloxane) on protein adsorption, platelet and cell adhesion. Colloids Surf B Biointerfaces. 2009;71:275-81.
[55] Kolandaivelu K, Swaminathan R, Gibson WJ, Kolachalama VB, Nguyen-Ehrenreich KL, Giddings VL, et al. Stent thrombogenicity early in high-risk interventional settings is driven by stent design and deployment and protected by polymer-drug coatings. Circulation. 2011;123:1400-9.
[56] Vaquette C, Cooper-White JJ. Increasing electrospun scaffold pore size with tailored collectors for improved cell penetration. Acta Biomaterialia. 2011;7:2544-57.
[57] Cui W, Li X, Zhou S, Weng J. Degradation patterns and surface wettability of electrospun fibrous mats. Polym Degr Stabil. 2007;93(3):731-8.
[58] Alberts B, Johnson A, Lewis J, Raff M, Roberts K, Walter P. Molecular Biology of the Cell. New York: Garland Science; 2002.
[59] Balguid A, Mol A, van Marion MH, Bank RA, Bouten CV, Baaijens FP. Tailoring fiber diameter in electrospun poly(epsilon-caprolactone) scaffolds for optimal cellular infiltration in cardiovascular tissue engineering. Tissue Eng Part A. 2009;15:437-44.
[60] Zhong S, Zhang Y, Lim CT. Fabrication of Large Pores in Electrospun Nanofibrous Scaffolds for Cellular Infiltration: A Review. Tissue Eng Part B Rev. 2011.
[61] Tian F, Hossinkhani H, Yokoyama Y, Gomes Estrada G, Kobayashi H. The effect of siameter of electrospun PGA scaffold for biological behavior of human umbilical endothelial cells. Key Engineering Materials. 2007;342-343:237-40.
[62] Soliman S, Sant S, Nichol JW, Khabiry M, Traversa E, Khademhosseini A. Controlling the porosity of fibrous scaffolds by modulating the fiber diameter and packing density. J Biomed Mater Res A.

Table 1: Electrospinning parameters used for the production of the different DegraPol and PLGA fibrous-scaffolds. The concentration represents the weight portion of polymer in the solvent mixture (25% HFP and 75% Chloroform was used for DegraPol and pure Chloroform was used for PLGA).

Polymer	Scaffold	Concentration	Flow rate	Working distance	Applied voltage
DegraPol	ES1	15 %	0.1 mL/h	25 cm	5 kV
	ES2	25 %	0.4 mL/h	20 cm	10 kV
	ES3	25 %	1 mL/h	15 cm	15 kV
PLGA	ES1	15 %	0.4 mL/h	25 cm	10 kV
	ES2	25 %	1 mL/h	20 cm	10 kV
	ES3	25 %	1.5 mL/h	15 cm	10 kV

Table 2: Water contact angle measurements of the polymeric scaffolds.

Polymer	Scaffold	Water Contact Angle [°]
DegraPol	CS	73.1 ± 2.6
	ES1	128.6 ± 4.2
	ES2	116.3 ± 5.3
	ES3	118.7 ± 1.9
PLGA	CS	76.6 ± 13.1
	ES1	122.8 ± 3.5
	ES2	117.5 ± 5.9
	ES3	118.5 ± 2.4

Figure legends

Figure 1: SEM Micrographs of the DP (a-d) and PLGA (e-h) scaffolds. Electrospun scaffolds with different fiber diameter ES1-3 (b-e and f-h), and the films used as controls CS (a and e). Bar = 20 µm. Mean fiber diameters (i) and pore areas (j) of the scaffolds are shown (no values were reported for the film CS). k) represents a graph of the pore area compared to the fiber diameter on which the dashed line is a quadratic trend line with corresponding R^2 value. Asterisks indicate statistical significance ($p > 0.05$) between the two scaffolds classes, while no significant differences were found comparing DP scaffolds to PLGA ones.

Figure 2: False-color images indicating the surface topography of the DegraPol (a-d) and PLGA (e-h) surfaces. The images were obtained from stereo-pairs form SEM images reconstructed with MeX (Alicona), and used for calculation of surface roughness. Scaffold roughness (Ra) is shown in i. j) represents a graph of the scaffold roughness compared to the fiber diameter on which the dashed line is a linear trendline with corresponding R^2 value. Asterisks indicate statistical significance ($p > 0.05$) between the two scaffolds classes, while no significant differences were found comparing DP scaffolds to PLGA.

Figure 3: Immunofluorescence micrographs of cast (a and e) and electrospun (b-d and f-h) DegraPol (a-d) and PLGA (e-h) scaffolds after exposure to partially heparinized whole human blood for 2 hrs at 37°C. Surfaces were stained with Hoechst (blue) for nuclei, with

phalloidin-Alexa 488 conjugate (green) for actin and with anti-CD62p (red) for activated platelets. i) represents a quantification of surface coverage by blood cells as determined after staining the actin cytoskeleton. j) Represents surface coverage of CD62p-positive-activated platelets. Bar = 50 µm. Asterisks indicate statistical significance ($p > 0.05$) between the two.

Figure 4: TAT levels in 3 IU heparin/mL whole blood after 2 hours incubation with the polymeric scaffolds. The dotted line surrounded by the gray area represent the mean TAT levels in blood before incubation and its deviation while the dashed line and the surrounding area represents the mean TAT levels in blood after incubation with a highly thrombogenic Titanium surface and deviation.

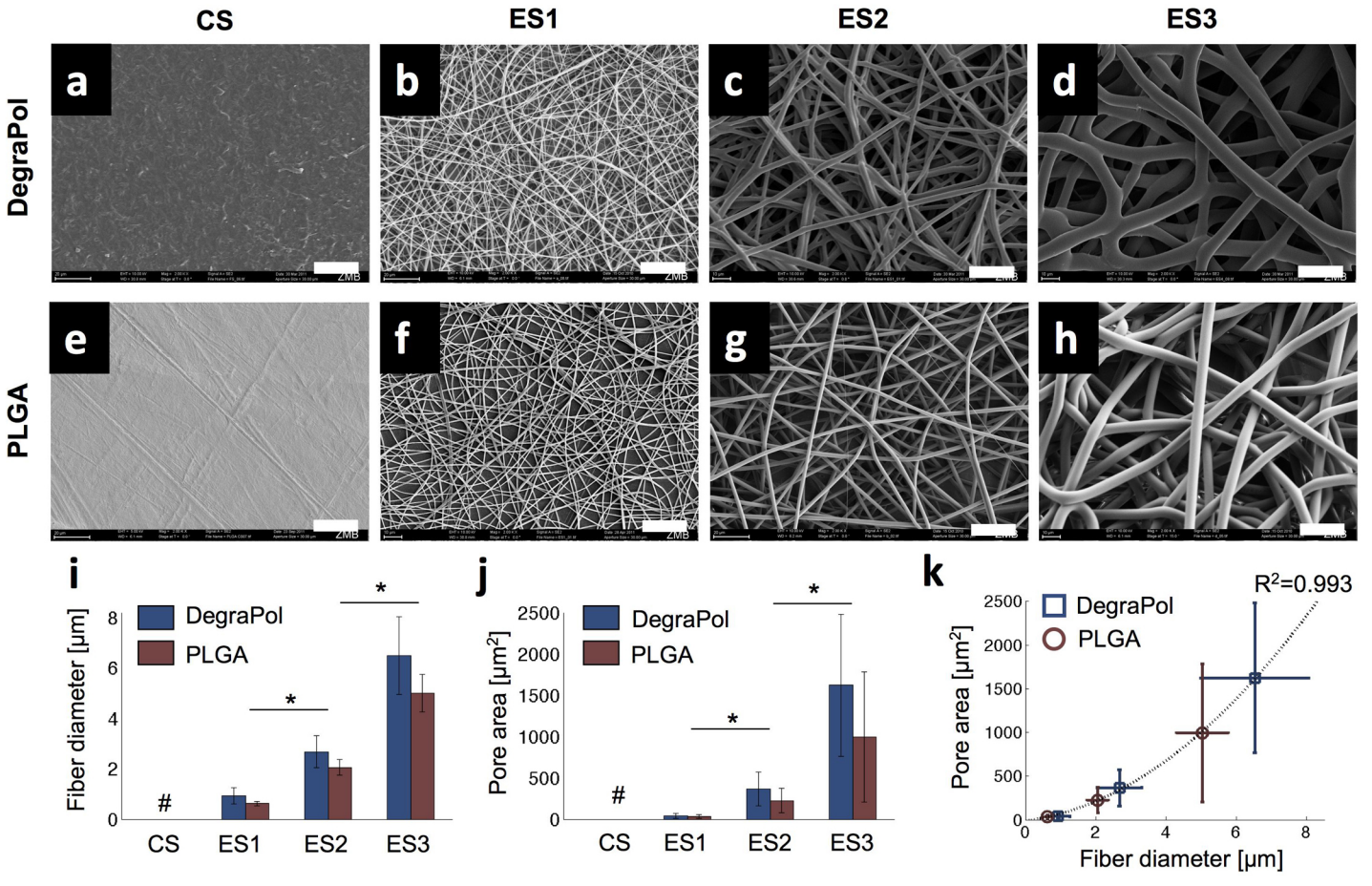
CS
ES1
ES2
ES3
DegraPol
PLGA
a
b
c
d
e
f
g
h
i
Fiber diameter [µm]
DegraPol
PLGA
#
*
*
CS
ES1
ES2
ES3
j
Pore area [µm²]
DegraPol
PLGA
#
*
*
CS
ES1
ES2
ES3
k
R²=0.993
DegraPol
PLGA
Pore area [µm²]
Fiber diameter [µm]

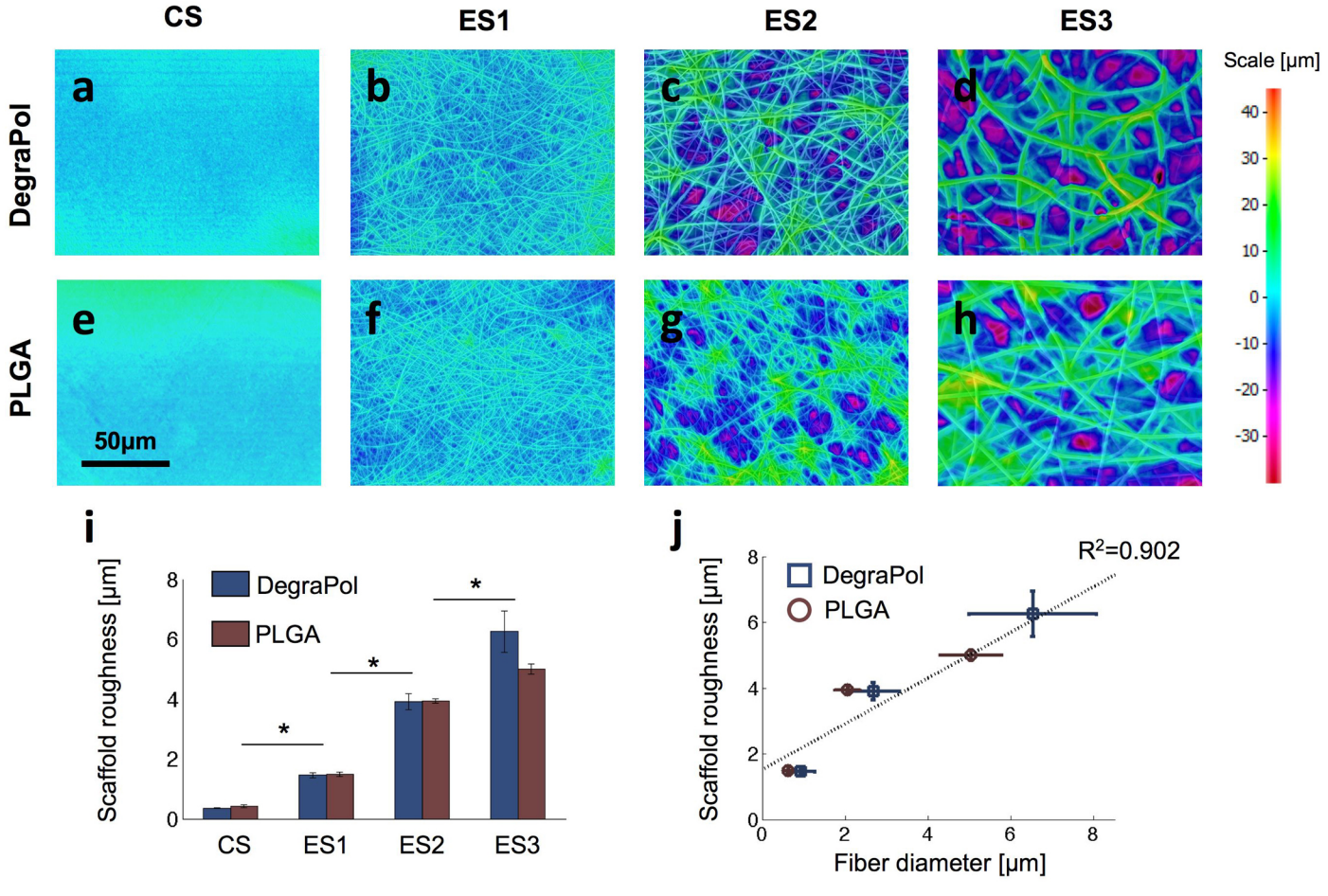
CS
ES1
ES2
ES3
DegraPol
PLGA
a
b
c
d
e
f
g
h
50µm
Scale [µm]
40
30
20
10
0
-10
-20
-30
i
Scaffold roughness [µm]
DegraPol
PLGA
*
*
*
0
2
4
6
8
CS
ES1
ES2
ES3
j
Scaffold roughness [µm]
R²=0.902
DegraPol
PLGA
0
2
4
6
8
Fiber diameter [µm]

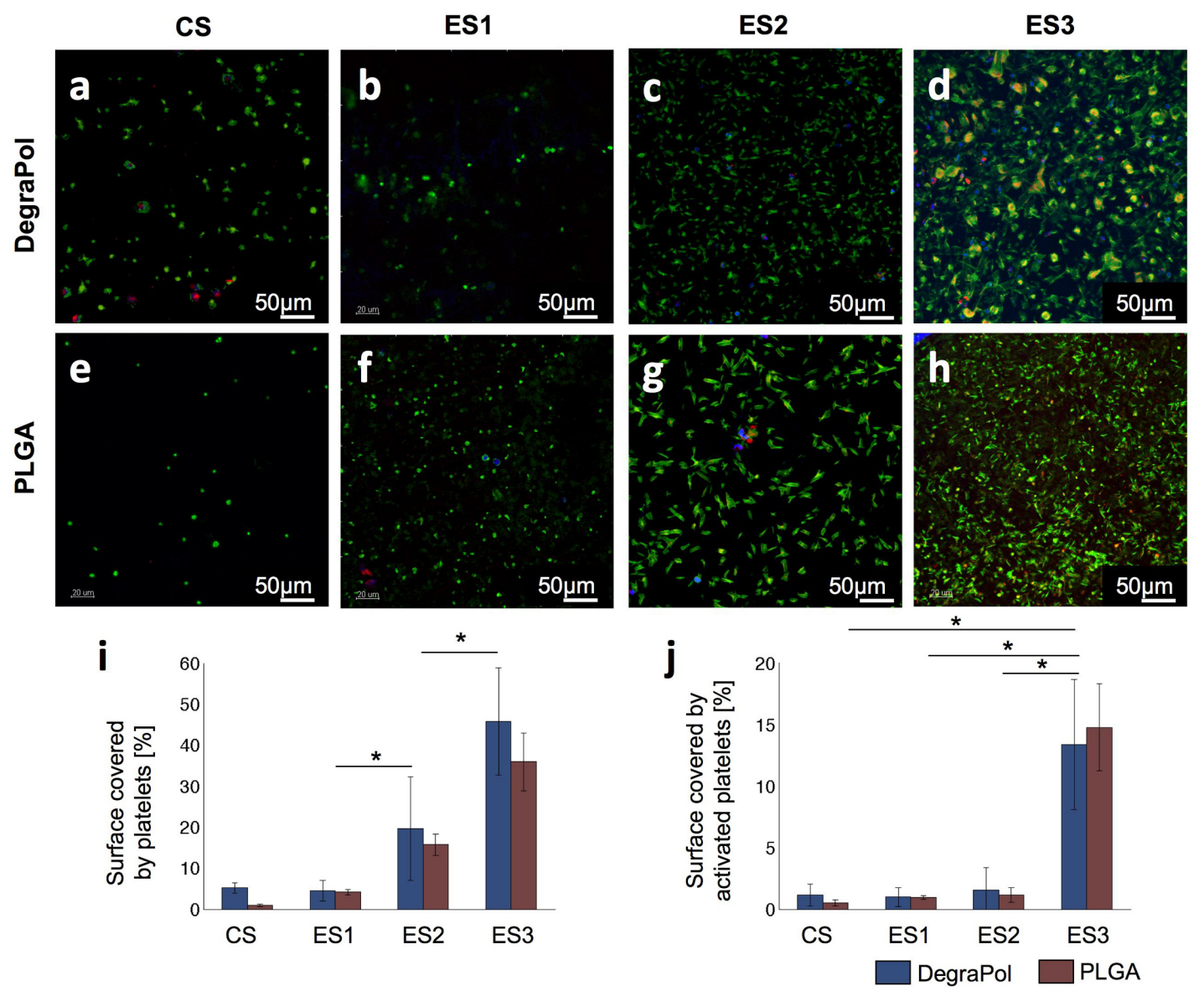
CS
ES1
ES2
ES3
DegraPol
PLGA
a
b
c
d
e
f
g
h
50µm
20 um
i
Surface covered by platelets [%]
60
50
40
30
20
10
0
*
*
CS
ES1
ES2
ES3
j
Surface covered by activated platelets [%]
20
15
10
5
0
*
*
*
CS
ES1
ES2
ES3
DegraPol
PLGA

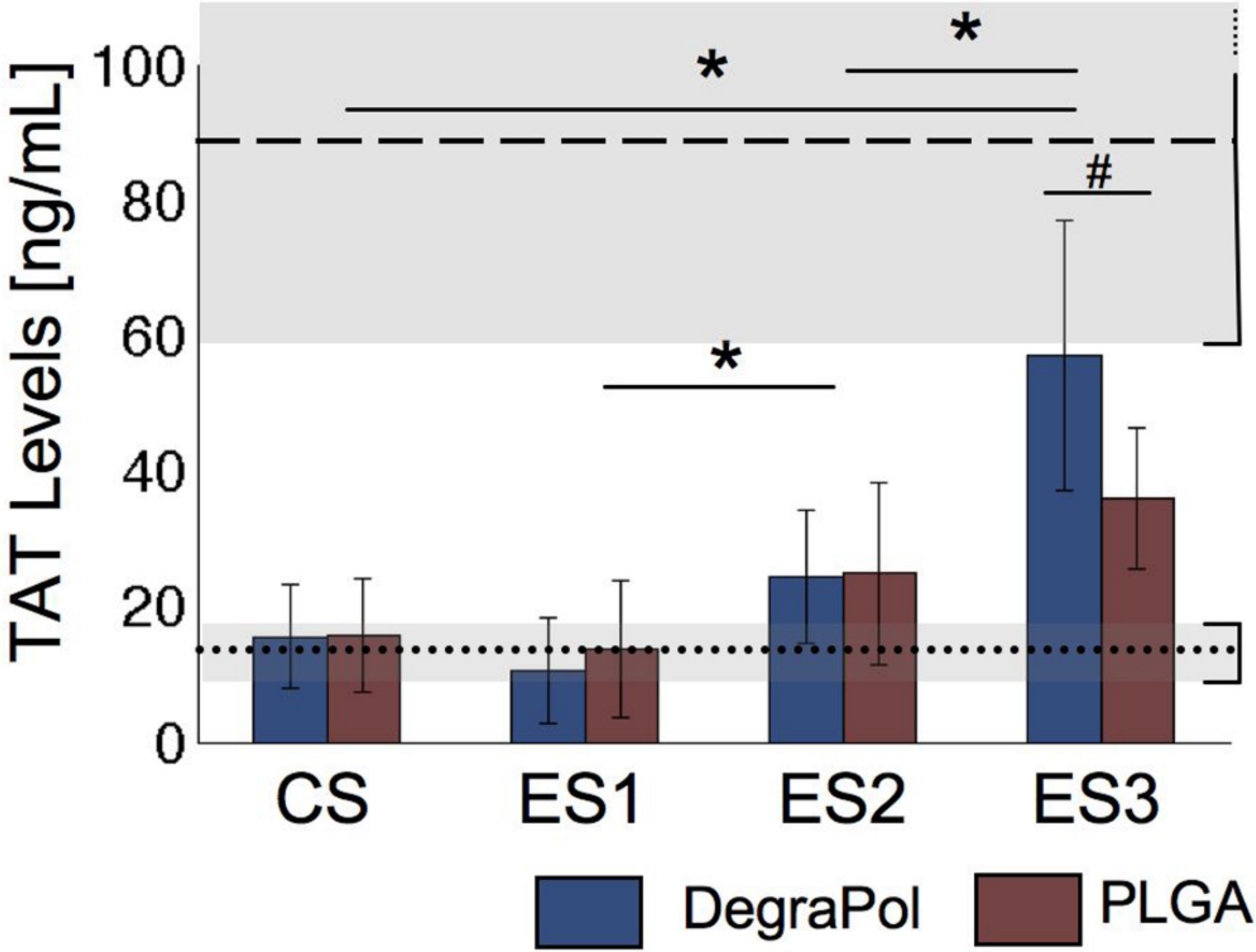
TAT Levels [ng/mL]
100
80
60
40
20
0
*
*
*
#
*
CS
ES1
ES2
ES3
DegraPol
PLGA